catalysts

MDPI

Article

Hall Current and Soret Effects on Unsteady MHD Rotating Flow of Second-Grade Fluid through Porous Media under the Influences of Thermal Radiation and Chemical Reactions

Omar T Bafakeeh [1], Kodi Raghunath [2], Farhan Ali [3], Muhammad Khalid [3], El Sayed Mohamed Tag-ElDin [4], Mowffaq Oreijah [5], Kamel Guedri [5,6], Nidhal Ben Khedher [7,8] and Muhammad Ijaz Khan [9,10,*]

1 Department of Industrial Engineering, Jazan University, Jazan 82822, Saudi Arabia
2 Department of Humanities and Sciences, Bheema Institute of Technology and Science, Adoni 518301, India
3 Department of Mathematical Sciences, Federal Urdu University of Arts, Sciences & Technology, Gulshan-e-Iqbal, Karachi 75300, Pakistan
4 Faculty of Engineering and Technology, Future University in Egypt, New Cairo 11835, Egypt
5 Mechanical Engineering Department, College of Engineering and Islamic Architecture, Umm Al-Qura University, Makkah 21955, Saudi Arabia
6 Research Unity: Materials, Energy and Renewable Energies, Faculty of Science of Gafsa, University of Gafsa, Gafsa 2100, Tunisia
7 Department of Mechanical Engineering, College of Engineering, University of Ha'il, Ha'il 81451, Saudi Arabia
8 Laboratory of Thermal and Energy Systems Studies, National School of Engineering of Monastir, University of Monastir, Monastir 5000, Tunisia
9 Department of Mathematics and Statistics, Riphah International University I-14, Islamabad 44000, Pakistan
10 Department of Mechanical Engineering, Lebanese American University, Beirut 1102, Lebanon
* Correspondence: mikhan@math.qau.edu.pk

Abstract: The unsteady MHD free convection heat and mass transfer flow of a viscous, incompressible, and electrically conducting fluid passing through a vertical plate embedded in a porous medium in the presence of chemical reactions and thermal radiation is investigated. The effects of the Hall current, rotation and Soret are studied. Using the perturbation approach, one can obtain an accurate analytical solution to the governing equations for the fluid velocity, fluid temperature, and species concentration, provided that the initial and boundary conditions are acceptable. It is possible to obtain expressions for the shear stress, rate of heat transfer, and rate of mass transfer for both plates with the ramping temperature and isothermal conditions. On the one hand, the numerical values of the primary and secondary fluid velocities, fluid temperature, and species concentration are presented graphically. On the other hand, the numerical values of the shear stress and rate of mass transfer for the plate are presented in tabular form for various values of the relevant flow parameters. These values are given for a range of pertinent flow parameters. It was determined that an increase in the Hall and Soret parameters over the whole fluid area leads to a corresponding increase in the resulting velocity. The resultant velocity continually climbs to a high level due to the contributions of the thermal and solute buoyancy forces. Lowering the heat source parameter reduces the temperature distribution, resulting in a lower overall temperature. When there is a rise in the chemical reaction parameter over the whole fluid area, there is a corresponding decrease in the concentration. The concentration buoyancy force, Hall current, and Prandtl number reduce the skin friction. On the other hand, the permeability of the porous medium, rotation, chemical reaction, the Soret number, thermal buoyancy force, and mass diffusion all have the opposite effects on the skin friction.

Keywords: Hall effect; chemical reaction; Soret effect; momentum boundary layer; thermal boundary layer; concentration boundary layer

Citation: Bafakeeh, O.T.; Raghunath, K.; Ali, F.; Khalid, M.; Tag-ElDin, E.S.M.; Oreijah, M.; Guedri, K.; Khedher, N.B.; Khan, M.I. Hall Current and Soret Effects on Unsteady MHD Rotating Flow of Second-Grade Fluid through Porous Media under the Influences of Thermal Radiation and Chemical Reactions. *Catalysts* **2022**, *12*, 1233. https://doi.org/10.3390/catal12101233

Academic Editors: Gregor Dionys Wehinger and Thomas Eppinger

Received: 28 August 2022
Accepted: 10 October 2022
Published: 14 October 2022

1. Introduction

In several subfields of geophysics, astrophysics, and fluid engineering, theoretical and practical studies of the hydromagnetic natural convection flow in a rotating medium,

considering the effects of radiation, are of significant interest. In light of this, Bestman and Adjepong [1] investigated the unsteady hydromagnetic free convection flow of an incompressible, optically thick liquid with radiative heat transfer near a moving flat plate in a rotating medium by imposing a time-dependent perturbation on a plate temperature that remained constant. They achieved this by simulating the fluid flow near the plate as it rotated. Mbeledogu and Ogulu [2] investigated the heat and mass transfer of the unsteady MHD natural convection flow of a rotating fluid through a vertical porous plate in the presence of radiative heat transfer. They focused their attention on the effects of the radiative heat transfer. They used the Rosseland assumption for an optically thick fluid so as to describe the radiative flux. Recently, Seth et al. [3] examined the effects of thermal radiation and rotation on the unsteady hydromagnetic free convection flow through an impulsively moving vertical plate with a ramping temperature in a porous medium. They achieved this by considering how these factors influenced the flow. It has been observed that the Hall current plays a crucial role in defining the flow characteristics of a fluid flow [4] when the density of the electrically conducting fluid is low and the applied magnetic field is high. It is essential to remember that the Hall current and rotation both cause a secondary flow to be produced in the flow field. Sarkar et al. [5] investigated the effects of Hall current on the unsteady MHD free convective flow behind an accelerated moving vertical plate with viscous and Joule dissipations. Anjali Devi and colleagues [6] studied the unsteady MHD free convection flow across an impulsively moving porous plate with viscous and Joule dissipations. Researchers Farhad et al. [7] examined the impacts of Hall current on an unsteady hydromagnetic rotating flow through a moving plate with an unlimited number of pores while the vessel was in a porous medium in a slip state. Raghunath and Mohanaramana [8] researched the Hall, Soret, and rotational effects on an unsteady MHD rotating flow of a second-grade fluid through a porous media when a chemical reaction and an aligned magnetic field were also present. The Hall and ion slip radiative flow of a chemically reactive, second-grade fluid through a porous saturated space was investigated by Raghunath et al. [9] using a perturbation technique. The development of the heat and mass transport in the presence of Hall, ion slip, and thermos-diffusion in a radiative second-grade material was recently investigated by Deepthi et al. [10].

The study of how thermal radiation influences the flow and heat transfer has become more significant in the industrial sector. At high temperatures, there is potential for considerable changes to occur in both the heat transfer and temperature profiles of micropolar fluids across a variety of geometries, as indicated in a study by Battacharyya et al. [11]. The effects of radiation on the thermal boundary layer flow of a micropolar fluid moving toward a permeable stretching sheet were studied by Hussain et al. [12]. Oahimire and Olajuwon [13] examined the impacts of the Hall current and thermal radiation on the heat and mass transfer of the chemically reacting MHD flow of a micropolar fluid through a porous material. Mabood et al. [14] investigated the impacts of a nonuniform heat source/sink and Soret on an MHD non-Darcian convective flow of a micropolar fluid in the presence of radiation when the flow was observed to occur past a stretched sheet. The effects of the Soret, rotation, Hall, and ion slip on the unsteady MHD flow of a Jeffrey fluid through a porous medium in the presence of heat absorption and chemical reactions were investigated by Raghunath et al. [15]. The unsteady MHD convective flow of a Newtonian fluid passing through an inclined plate in the presence of chemical reactions with radiation absorption and Dufour effects was examined by Obulesu et al. [16]. Nagesh and Raghunath [17] examined the impacts of Soret radiation and chemical reactions on MHD Jeffrey fluid flow when it was directed via an inclined plate embedded in porous media.

Additionally, due to its many practical uses in the chemical and hydrometallurgical industries, the study of the heat and mass transfer flow in the presence of chemical reactions has garnered a significant amount of interest in recent years. Homogeneous and heterogeneous chemical reactions are the two most common kinds of chemical reactions. If a chemical reaction takes place at an interface rather than in a single phase across its volume, it is referred to as a heterogeneous reaction rather than a homogeneous reaction.

A heterogeneous reaction takes place in a confined area or inside the border of a phase, in contrast to a homogeneous reaction, which takes place evenly over the entire the given phase. melting, the production of ceramics and glassware, catalytic chemical reactors, the production polymers, the manufacturing of ceramics and glassware, and the initiation of exothermic or endothermic chemical reactions are just some of the numerous important applications of heat and mass transfer flows with chemical reactions. There are a great number of other important applications as well. A number of researchers, mindful of the importance of this kind of study, have examined the hydromagnetic free convection heat and mass transfer flow of a viscous, incompressible, and electrically conducting fluid moving past a vertical plate in the presence of a first-order chemical reaction under a variety of different conditions. The means by which a chemical reaction, with suction, might impact an isothermal moving vertical surface was investigated by Muthucumaraswamy [18]. Ajibade et al. [19] discussed the impact of a chemical reaction on the erratic hydromagnetic natural convective coquette flow in a vertical channel packed with porous materials. Recently, the authors of [20–25] investigated how different flow geometries are impacted by chemical interactions.

The essential engineering implementations for an MHD boundary layer flow with heat transfer include the consequences of Hall current. These applications are found in MHD power generators and pumps, Hall accelerators, refrigeration coils, electric transformers, in-flight MHD, solar physics involved in the development of sunspots, the solar cycle, the structure of magnetic stars, electronic system cooling, cool combustors, fiber and granular insulation, oil extraction, thermal energy storage, and fluorohydrodynamics (flooding). Satya Narayana and colleagues [26] investigated the effects of Hall current and the radiation–absorption process on the MHD natural convection heat and mass transfer flow of a micropolar fluid in a rotating frame of reference. Seth et al. [27] investigated the effects of Hall current and the rotation on the unsteady hydromagnetic natural convection flow of a viscous, incompressible, electrically conducting, and heat-absorbing fluid moving past an impulsively moving vertical plate with a ramped temperature in a porous medium. They also took into account the effect of thermal diffusion. Seth et al. [28] studied the effects of the Hall current, thermal radiation, and rotation on the natural convection heat and mass transfer flow flowing past a moving vertical plate. Takhar et al. [29] examined the influence of Hall current on the MHD flow over a moving plate in a fluid that rotates with a magnetic field and has a free stream velocity.

The focus of the current investigation is the analysis of the effects of the Hall current and rotation and the Soret effect on the unsteady MHD free convection flow of a viscous, incompressible, electrically conducting fluid moving past an impulsively movable vertical plate in a porous medium in the presence of thermal radiation and chemical processes. This investigation was carried out in the presence of thermal radiation and chemical reactions. A general solution is produced, firstly, by transforming the governing equations into a set of normalized equations, and then solving the equations analytically using the perturbation method, thereby obtaining the answer. The effects of the various parameters on the fluid velocity, temperature, and concentration distributions are plotted and discussed. These parameters include the magnetic field parameter, Schmidt number, Prandtl number, and Grashof number for the heat transfer and mass transfer, chemical reactions, thermal radiation, Hall current, rotation, and Soret effect.

2. Formulation of the Problem

The coordinate system is selected so that the x-axis is assumed to be situated along the plate in the upward direction, and the y-axis is regarded to be normal to the plate's plane when immersed in the fluid. The application of a uniform transverse magnetic field, denoted as B0, is performed in the perpendicular direction to the y-axis. The fluid and the plate spin are in the same direction around the y-axis, with the same constant angular velocity. The temperature at the surface of the plate is raised to the desired uniform temperature, and the concentration of species on the surface of the plate is raised to

the desired uniform concentration before being maintained at that level afterward. The geometry of the problem can be seen in Figure 1. All physical parameters, except for the pressure, depend solely on y and t. This is because the plate has an unlimited extension in both the x and z directions and does not conduct electricity. Because there are neither applied voltages nor polarized voltages, the impact of polarization on the fluid is essentially null. In this scenario, no electrical energy is either contributed to or withdrawn from the liquid in question. The induced magnetic field produced by the velocity of the fluid is insignificant in contrast to the magnetic field applied. This presumption is reasonable, since the magnetic Reynolds number is relatively low for partly ionized fluids and liquid metals, which are often used in various industrial applications.

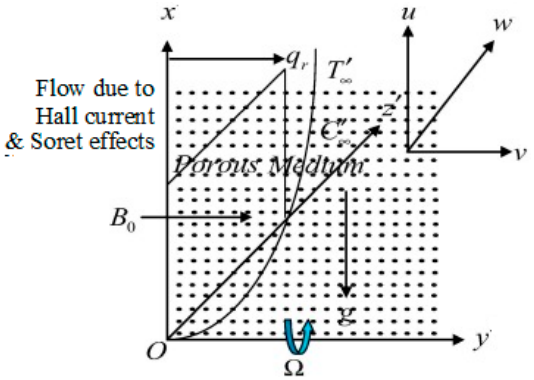

Figure 1. The geometry of the problem.

Keeping in mind the statements mentioned above, the governing equations for the natural convection flow of an electrically manipulating, viscous, incompressible liquid via an infinite upright plate implanted in a homogeneous permeable medium in a revolving system with heat and mass transfer are provided [10] by:

$$\frac{\partial u}{\partial x} + \frac{\partial v}{\partial y} = 0 \tag{1}$$

$$\frac{\partial u}{\partial t} + w\frac{\partial u}{\partial z} - 2\,\Omega\, v = -\frac{1}{\rho}\frac{\partial p}{\partial x} + v\frac{\partial^2 u}{\partial z^2} + \frac{\alpha}{\rho}\frac{\partial^3 u}{\partial z^2 \partial t} + \frac{B_0\, J_y}{\rho} + g\beta(T - T_\infty) + g\beta^*(C - C_\infty) - \frac{v}{k}\, u \tag{2}$$

$$\frac{\partial v}{\partial t} + w\frac{\partial v}{\partial z} + 2\,\Omega\, u = -\frac{1}{\rho}\frac{\partial p}{\partial y} + v\frac{\partial^2 v}{\partial z^2} + \frac{\alpha}{\rho}\frac{\partial^3 v}{\partial z^2 \partial t} - \frac{B_0\, J_x}{\rho} - \frac{v}{k}v \tag{3}$$

$$\frac{\partial T}{\partial t} + w\frac{\partial T}{\partial z} = \frac{k_1}{\rho C_p}\frac{\partial^2 T}{\partial z^2} - \frac{Q_0}{\rho C_p}(T - T_\infty) - \frac{1}{\rho C_p}\frac{\partial q_r}{\partial z} \tag{4}$$

$$\frac{\partial C}{\partial t} + w\frac{\partial C}{\partial z} = D\frac{\partial^2 C}{\partial z^2} - K_c(C - C_\infty) + D_1\frac{\partial^2 T}{\partial z^2} \tag{5}$$

Additionally, Equation (1) indicates the continuity equation, Equations (2) and (3) represent the momentum equation with the applied magnetic field and mixed convection assumptions, Equation (4) highlights the temperature equation subject to the thermal radiation and heat generation/absorption, and Equation (5) signifies the concentration equation with the chemical reaction effect.

The proper boundary conditions are provided by the aforementioned presumptions. In the case of the velocity distributions, thermodynamics and intensity:

$$u = U_0, \quad v = 0, \quad T = T_w + \varepsilon\,(T_w - T_\infty)e^{iwt}, \quad C = C_w + \varepsilon(C_w - C_\infty)e^{iw\,t} \quad \text{at } z = 0 \tag{6}$$

$$u \to U_\infty, \quad v \to 0, \quad T \to T_\infty \quad C \to C_\infty \quad \text{as} \quad z \to \infty \tag{7}$$

In mathematics, we take into account a formulation for a limit of optically thin grey gas that is close to the equilibrium in the specified form, by [30,31]:

$$\frac{\partial q_r*}{\partial y*} = 4(T^* - T_w^*)\ I \tag{8}$$

where $I = \int_0^\infty K_{\lambda\omega}\left(\frac{\partial_{eb\lambda}}{\partial T}\right)_\omega d\lambda$, and the absorbance factor at the wall, in addition to $eb\lambda$, is Planck's function.

We suppose, since the equation for continuity shows that w is either a constant or a time related function, that:

$$w = -w_0\ (1 + A\ \varepsilon\ e^{nt}) \tag{9}$$

where A is a constant that is actually positive. ε and $A\varepsilon$ are smaller than unity, and w_0 is the balance of the suction velocity with a non-zero positive constant. Suppose that the magnetic field has enormous strength. In that case, the exhaustive Ohms commandment to incorporate the Hall currents is unique. With the Hall currents assumed, the generalized Ohm's law [32] can be expressed as follows:

$$J + \frac{\omega_e\ \tau_e}{B_0}(J \times B) = \sigma\left[(E + V \times B) + \frac{1}{e\eta_e}\nabla P_e\right] \tag{10}$$

Furthermore, we presume that the electric field $E = 0$, under suppositions, diminishes to:

$$J_x + mJ_y = \sigma B_0\ v \tag{11}$$

$$J_y - mJ_x = -\sigma B_0 u \tag{12}$$

On solving Equations (11) and (12), we obtain:

$$J_x = \frac{\sigma B_0}{1 + m^2}(mu + v) \tag{13}$$

$$J_y = \frac{\sigma B_0}{1 + m^2}(mv - u) \tag{14}$$

Substituting Equations (13) and (14) for Equations (2) and (3), respectively, the resulting equations are:

$$\frac{\partial u}{\partial t} + w\frac{\partial u}{\partial z} - 2\ \Omega\ v = -\frac{1}{\rho}\frac{\partial p}{\partial x} + v\frac{\partial^2 u}{\partial z^2} + \frac{\alpha}{\rho}\frac{\partial^3 u}{\partial z^2 \partial t} + \frac{\sigma B_0}{\rho(1 + m^2)}(mv - u) + g\beta(T - T_\infty)\ + g\beta^*(C - C_\infty)\ - \frac{v}{k}u \tag{15}$$

$$\frac{\partial v}{\partial t} + w\frac{\partial v}{\partial z} + 2\ \Omega\ u = -\frac{1}{\rho}\frac{\partial p}{\partial y} + v\frac{\partial^2 v}{\partial z^2} + \frac{\alpha}{\rho}\frac{\partial^3 v}{\partial z^2 \partial t} - \frac{\sigma B_0}{\rho(1 + m^2)}(mu + v) - \frac{v}{k}v \tag{16}$$

Combining Equations (15) and (16), let $q = u + iv$ and $\xi = x - iy$. We obtain:

$$\frac{\partial q}{\partial t} - w\left(1 + \varepsilon A e^{nt}\right)\frac{\partial q}{\partial z} + 2i\ \Omega\ q = -\frac{1}{\rho}\frac{\partial p}{\partial \xi} + v\frac{\partial^2 q}{\partial z^2} + \frac{\alpha}{\rho}\frac{\partial^3 q}{\partial z^2 \partial t} - \frac{\sigma B_0}{\rho(1 - im)}q\ + g\beta(T - T_\infty\ )\ +\ g\beta^*(C - C_\infty) - \frac{1}{K}q \tag{17}$$

Outside the boundary layer, Equation (17) gives:

$$-\frac{1}{\rho}\frac{\partial p}{\partial \xi} = \frac{dU_\infty}{\partial t} + \frac{v}{k}U_\infty + \frac{\sigma B_0^2}{\rho}U_\infty \tag{18}$$

To uniformly express the physical problem mathematically, the subsequent non-dimensional quantities and parameters are provided:

$$\begin{gathered} q^* = \frac{q}{w_0}, w^* = \frac{w}{w_0},\ z^* = \frac{w_0\, z}{v},\ U_0^* = \frac{U_0}{w_0},\ U_\infty^* = \frac{U_\infty}{w_0},\ t^* = \frac{t}{v}\frac{w_0^2}{},\theta = \frac{T-T_\infty}{T_w-T_\infty}, \phi = \frac{C-C_\infty}{C_w-C_\infty}, \\ M^2 = \frac{\sigma\ B_0^2 v}{\rho w_0^2}, \Pr = \frac{v\ \rho C_p}{k_1} = \frac{v}{\alpha}, Sc = \frac{v}{D}, Gr = \frac{v g\beta(T_w-T_\infty)}{w_0^3}, Gm = \frac{v\ g\beta^*(C_w-C_\infty)}{w_0^3}, \\ k = \frac{w_0^2 k}{v^2},\ R = \frac{\Omega\ v}{w_0^2}, H = \frac{v\ Q_0}{\rho C_p w_0^2},\ S = \frac{w_0^2\ \alpha_1}{\rho\ v^2},\ K_c = \frac{K_c v}{w_0^2}, S_0 = \frac{D_1(T_w-T_\infty)}{w_0(C_w-C_\infty)},\ F = \frac{4I_1 v}{\rho C_p w_0^2} \end{gathered} \tag{19}$$

When reduced, the governing Equations (2)–(5) use non-dimensional variables:

$$\frac{\partial q}{\partial t} - (1 + A\varepsilon\, e^{nt})\frac{\partial q}{\partial z} = \frac{dU_\infty}{dt} + \frac{\partial^2 q}{\partial z^2} + S\frac{\partial^3 q}{\partial z^2 \partial t} - \left(\frac{M^2}{1-im} + 2iR + \frac{1}{k}\right) q + Gr\ \theta\ + Gm\ \ \phi \tag{20}$$

$$\frac{\partial \theta}{\partial t} - (1 + A\varepsilon e^{nt})\frac{\partial \theta}{\partial z} = \frac{1}{\Pr}\frac{\partial^2 \theta}{\partial z^2} - (H - F)\ \theta \tag{21}$$

$$\frac{\partial \phi}{\partial t} - (1 + A\varepsilon e^{nt})\frac{\partial \phi}{\partial z} = \frac{1}{Sc}\frac{\partial^2 \phi}{\partial z^2} - K_c\phi\ + S_0\frac{\partial^2 \theta}{\partial z^2} \tag{22}$$

The corresponding boundary conditions given are:

$$q = U_0, \quad \theta = 1 + \varepsilon\, e^{nt},\ \ \phi = 1 + \varepsilon e^{nt} \qquad \text{at}\ \ z = 0 \tag{23}$$

$$q = 0, \quad \theta = 0, \qquad \phi = 0 \qquad \text{as} \qquad z \to \infty \tag{24}$$

3. Solution of the Problem

A group of partial differential equations, represented by Equations (20) and (22), are not amenable to a closed-form solution. However, suppose they can be reduced to a set of analytically solvable differential equations in a dimensionless form. This can be achieved by representing the velocity, temperature, and concentration as follows:

$$q = q_0(z) + \varepsilon e^{nt} q_1(z) + O\left(\varepsilon^2\right) \tag{25}$$

$$\theta = \theta_0(z) + \varepsilon e^{nt} \theta_1(z) + O\left(\varepsilon^2\right) \tag{26}$$

$$\phi = \phi_0(z) + \varepsilon e^{nt} \phi_1(z) + O\left(\varepsilon^2\right) \tag{27}$$

Equations (25)–(27) are replaced by Equations (20)–(22), combining the harmonic and nonharmonic terms, ignoring the higher order terms of $O(\varepsilon^2)$. As a result, the following pair of equations are obtained:$(q_0, \theta_0, \phi_0)\ \ and (q_1, \theta_1, \phi_1)$

$$\frac{\partial^2 q_0}{\partial z^2} + \frac{\partial q_0}{\partial z} - \left[\frac{M^2}{1-im} + 2iR + \frac{1}{k}\right] q_0 = -Gr\ \theta_0\ - Gm\ \ \phi_0 \tag{28}$$

$$(1 + Sn)\frac{\partial^2 q_1}{\partial z^2} + \frac{\partial q_1}{\partial z} - \left[\frac{M^2}{1-im} + 2iR + \frac{1}{k} + n\right] q_1 = -Gr\ \theta_1\ - Gm\ \ \phi_1 - A\frac{\partial q_0}{\partial z} \tag{29}$$

$$\frac{\partial^2 \theta_0}{\partial z^2} + \Pr\frac{\partial \theta_0}{\partial z} - (H - F)\Pr\ \theta_0 = 0 \tag{30}$$

$$\frac{\partial^2 \theta_1}{\partial z^2} + \Pr\frac{\partial \theta_1}{\partial z} - (H - F + n)\ \Pr\ \theta_1 = -A\Pr\frac{\partial \theta_0}{\partial z} \tag{31}$$

$$\frac{\partial^2 \phi_0}{\partial z^2} + Sc\frac{\partial \phi}{\partial z} - Sc\ Kc\ \phi_0 = Sc\ So\ \frac{\partial^2 \theta_0}{\partial z^2} \tag{32}$$

$$\frac{\partial^2 \phi_1}{\partial z^2} + Sc\frac{\partial \phi_1}{\partial z} - (n + K_c)Sc\,\phi_1 = -\left(A\,\frac{\partial \phi_0}{\partial z} + So\frac{\partial^2 \theta_0}{\partial z^2}\right)Sc \tag{33}$$

The corresponding boundary conditions are:

$$\begin{array}{lll} q_0 = U_0,\ q_1 = 0, \quad \theta_0 = 1, \quad \theta_1 = 1,\ \phi_0 = 1\ ,\ \phi_1 = 0 & & \text{at } z = 0 \\ q_0 = 0,\ q_1 = 0, \quad \theta_0 = 0, \quad \theta_1 = 0,\ \phi_0 = 0,\ \phi_1 = 0 & \text{as} & z \to \infty \end{array} \tag{34}$$

Solving Equations (28)–(33) under the boundary conditions of Equation (34), we discover the field of velocity, temperature, and concentration:

$$\begin{array}{l} q(z,t) = b_9 \exp(-m_1 z) + b_{10} \exp(-m_3 z) + b_{11} \exp(-m_5 z) + \\ \qquad \varepsilon e^{nt} \left(\begin{array}{l} b_{12} \exp(-m_1 z) + b_{13} \exp(-m_2 z) + b_{14} \exp(-m_3 z) + \\ b_{15} \exp(-m_4 z) + \ \ b_{16} \exp(-m_5 z) + b_{17} \exp(-m_6 z) \end{array} \right) \end{array} \tag{35}$$

$$\theta(z,t) = \exp(-m_1 z)\ + \varepsilon e^{nt}(b_1 \exp(-m_1 z) + b_2 \exp(-m_2 z)) \tag{36}$$

$$\varphi(z,t) = b_1 \exp(-m_1 z) + b_4 \exp(-m_3 z) + \varepsilon e^{nt}(b_5 \exp(-m_1 z) + b_6 \exp(-m_2 z) + b_7 \exp(-m_3 z) + b_8 \exp(-m_4 z)) \tag{37}$$

3.1. Skin Friction

The skin friction, which is presented in a non-dimensional form and is derived as follows, is an essential quantity in terms of the physical state of the boundary:

$$\tau = \left(\frac{\partial u}{\partial y}\right)_{y=0} = -\left((b_9 m_1 + b_{10} m_3 + b_{11} m_5) + \ \varepsilon e^{nt} \left(\begin{array}{c} b_{12} m_1 + b_{13} m_2 + \\ b_{14} m_3 + b_{15} m_4 + \ \ b_{16} m_5 + b_{17} m_6 \end{array} \right)\right) \tag{38}$$

3.2. Nusselt Number

Another physical quantity, such as the rate of heat transfer, is represented as the Nusselt number by:

$$Nu = -\left(\frac{\partial \theta}{\partial y}\right)_{y=0} = m_1 + \varepsilon e^{nt}(b_1 m_1 + b_2 m_2\ ) \tag{39}$$

3.3. Sherwood Number

Additionally, the rate of mass transfer can be expressed as the Sherwood number, which can be determined by:

$$Sh = -\left(\frac{\partial C}{\partial y}\right)_{y=0} = \left((b_1 m_1 + b_4 m_3) + \varepsilon e^{nt}(b_5 m_1 + b_6 m_2 + b_7 m_3 + b_8 m_4)\right) \tag{40}$$

4. Results and Discussion

The preceding sections employed the perturbation approach to analytically solve the governing equations and boundary conditions. Finally, the suitable non-dimensional flow parameter's effects on the primary (u) and secondary (v) velocity, temperature (θ), and concentration(φ) distribution were obtained. This includes both graphic representations of non-dimensional quantities, as well as tabular representations of non-dimensional quantities. In Figures 2–9, we take M = 2.0, k = 0.50, Gr = 5.0, S = 1.0, Gm = 3.0, R = 1.0, m = 0.20, Pr = 0.710, H = 1.0, Sc = 0.220, Kc = 1.0, n = 0.50, t = 0.50, F = 1.0. The authors of [33–38] described some important investigations regarding mathematical techniques and nano concepts.

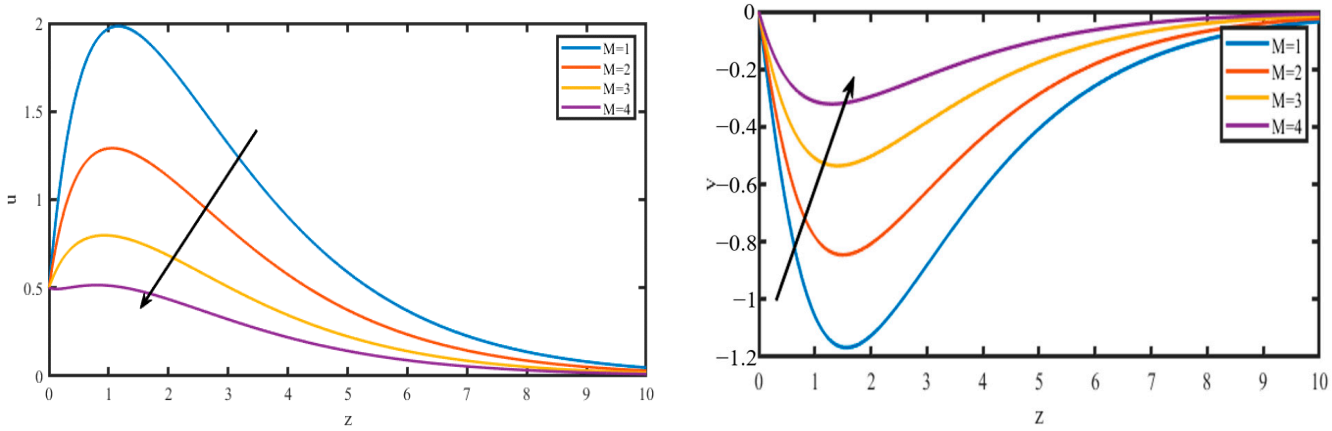

Figure 2. The velocity patterns for u and v plotted vs. M, with k = 0.50, R = 1.0, Gr = 5.0, S = 1.0, Gm = 3.0, m = 0.20, Pr = 0.710, H = 1.0, Sc = 0.220, Kc = 1.0, n = 0.50, t = 0.50, So = 0.50, F = 1.0.

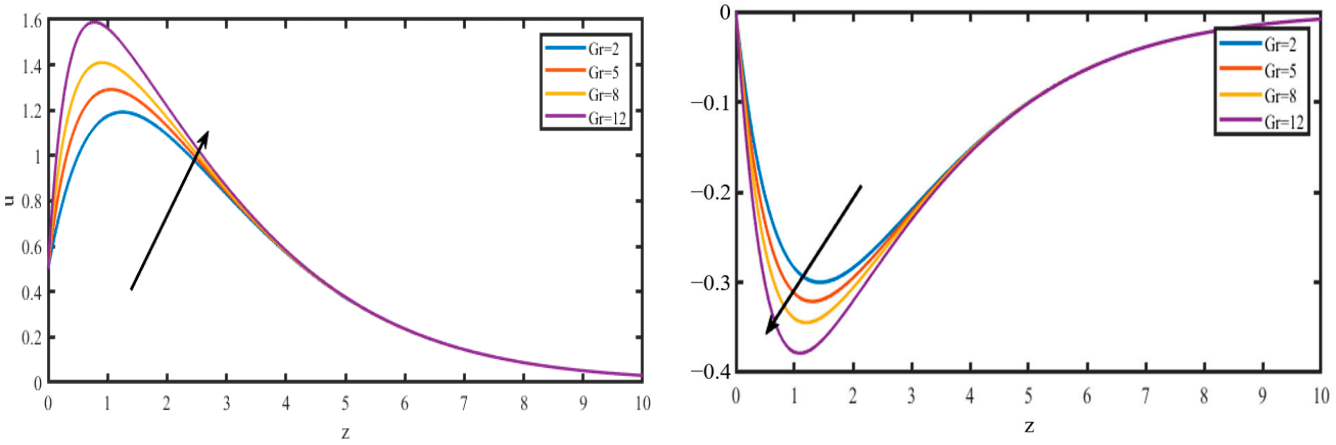

Figure 3. The velocity patterns for u and v plotted vs. Gr, with k = 0.50, R = 1.0, M = 2.0, S = 1.0, Gm = 3.0, m = 0.20, Pr = 0.710, H = 1.0, Sc = 0.220, Kc = 1.0, n = 0.50, t = 0.50, So = 0.50, F = 1.0.

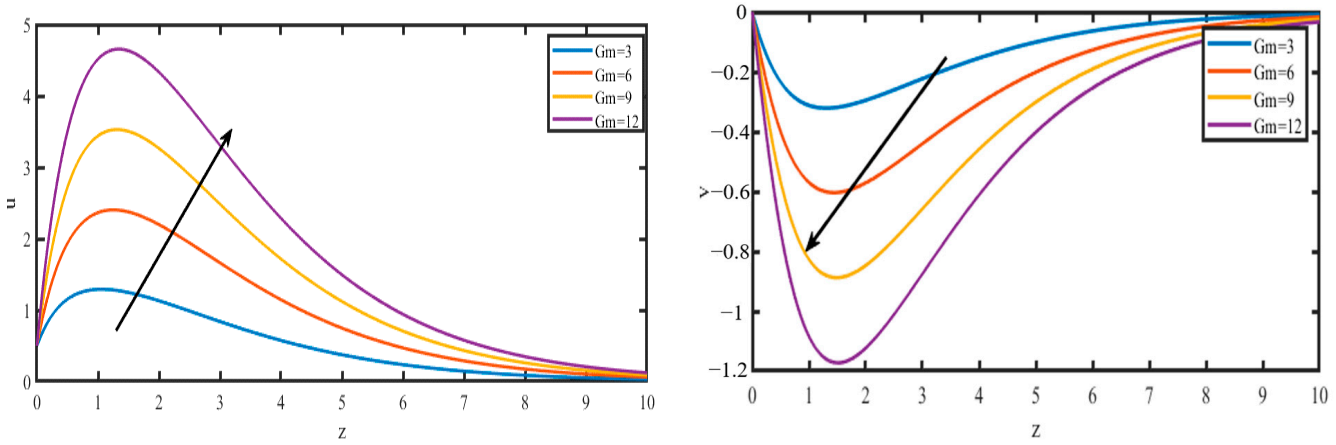

Figure 4. The velocity patterns for u and v plotted vs. Gm, with k = 0.50, R = 1.0, Gr = 5.0, S = 1.0, M = 2.0, m = 0.20, Pr = 0.710, H = 1.0, Sc = 0.220, Kc = 1.0, n = 0.50, t = 0.50, So = 0.50, F = 1.0.

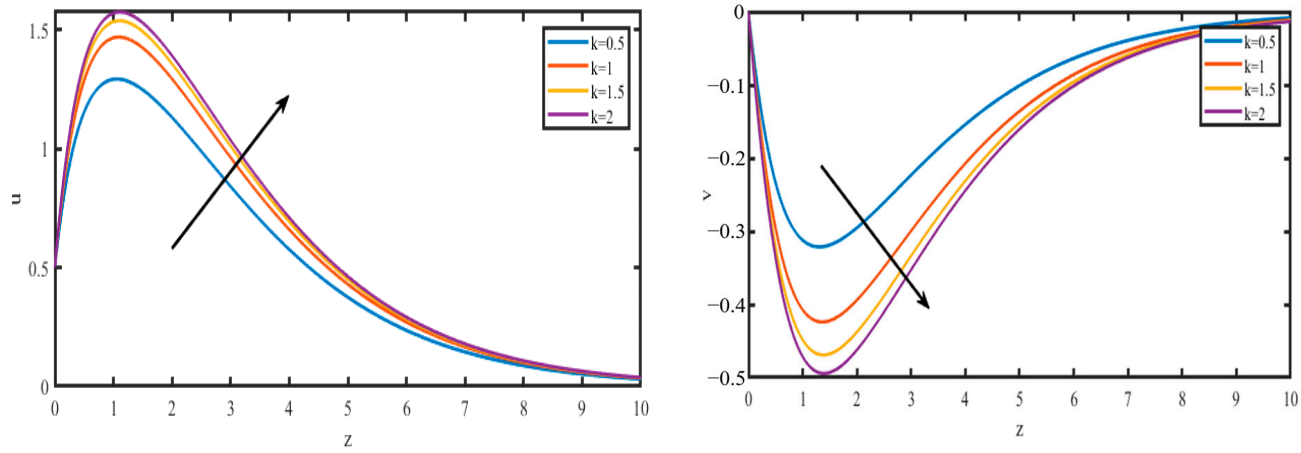

Figure 5. The velocity patterns for u and v plotted vs. k, with M = 2.0, R = 1.0, Gr = 5.0, S = 1.0, Gm = 3.0, m = 0.20, Pr = 0.710, H = 1.0, Sc = 0.220, Kc = 1.0, n = 0.50, t = 0.50, So = 0.50, F = 1.0.

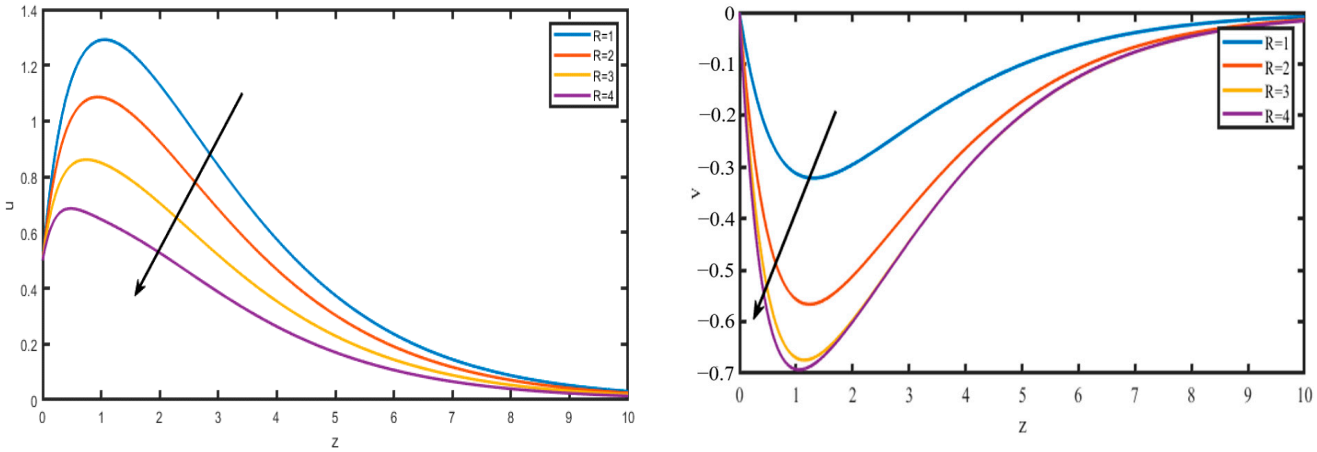

Figure 6. The velocity patterns for u and v plotted vs. R, with k = 0.50, M = 2.0, Gr = 5.0, S = 1.0, Gm = 3.0, m = 0.20, Pr = 0.710, H = 1.0, Sc = 0.220, Kc = 1.0, n = 0.50, t = 0.50, So = 0.50, F = 1.0.

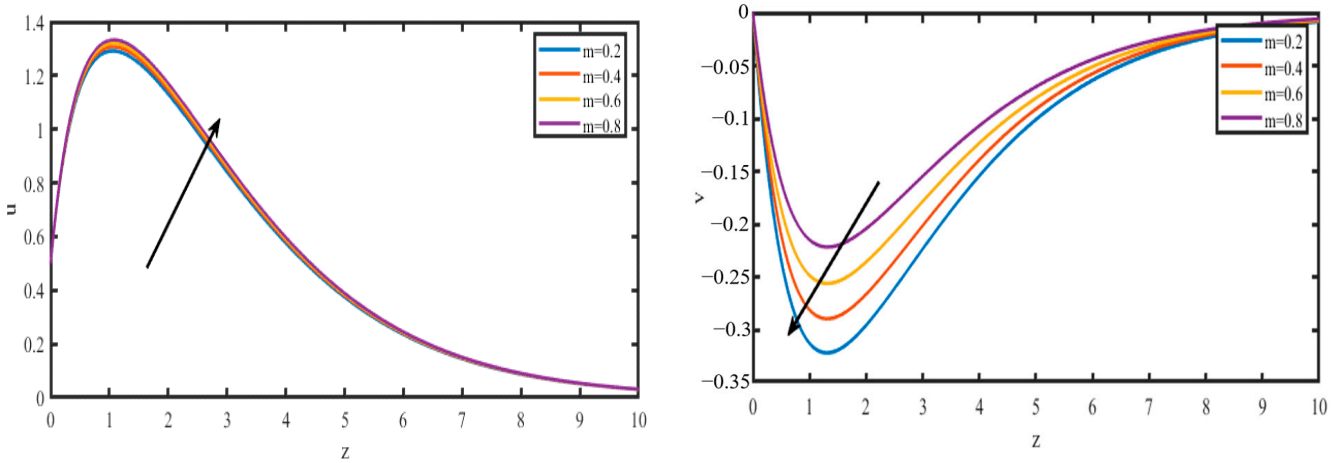

Figure 7. The velocity patterns for u and v plotted vs. m, with k = 0.50, R = 1.0, Gr = 5.0, S = 1.0, Gm = 3.0, M = 2.0, Pr = 0.710, H = 1.0, Sc = 0.220, Kc = 1.0, n = 0.50, t = 0.50, So = 0.50, F = 1.0.

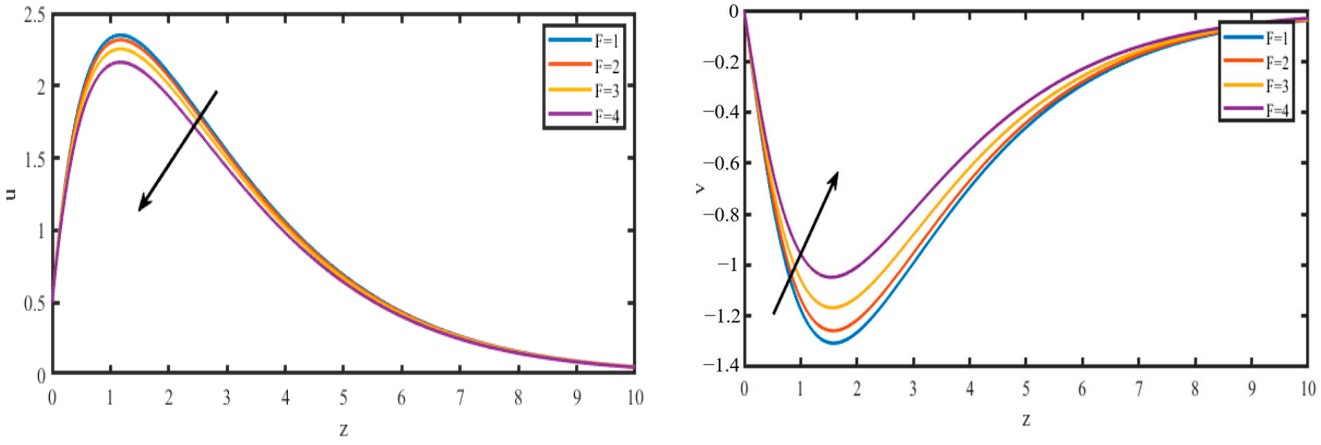

Figure 8. The velocity patterns for u and v plotted vs. F, with k = 0.50, R = 1.0, Gr = 5.0, S = 1.0, Gm = 3.0, m = 0.20, Pr = 0.710, H = 1.0, Sc = 0.220, Kc = 1.0, n = 0.50, t = 0.50, So = 0.50, M = 2.0.

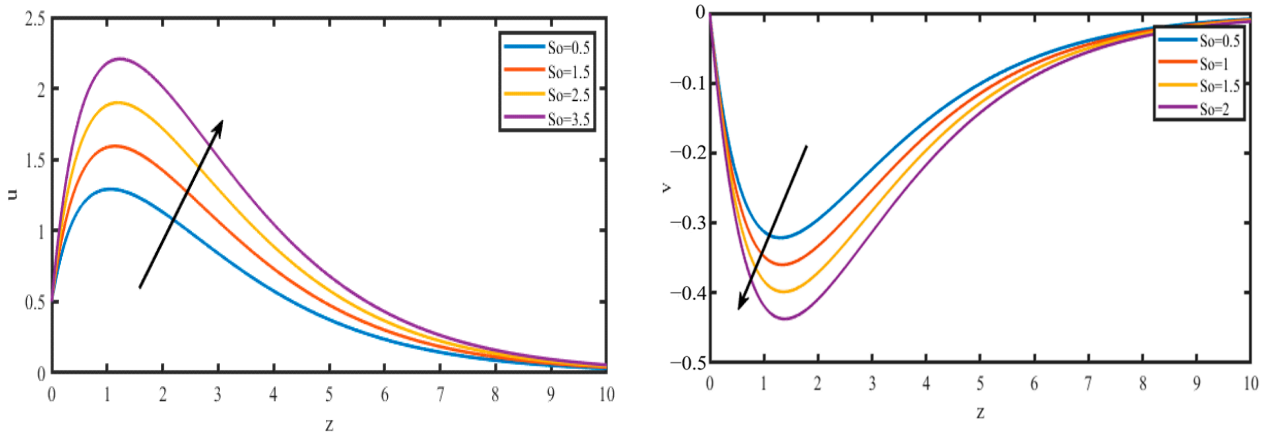

Figure 9. The velocity patterns for u and v plotted vs. So, with k = 0.50, R = 1.0, Gr = 5.0, S = 1.0, Gm = 3.0, m = 0.20, Pr = 0.710, H = 1.0, Sc = 0.220, Kc = 1.0, n = 0.50, t = 0.50, M = 2.0, F = 1.0.

Figure 2 explains the significance of the Hartmann digit M for the various velocity components. After enhancing the values of Hartmann number, the velocity profile and its associated boundary layer declines. Because of the Hall current's effect on the entire fluid region, the velocity component v increases. A reduction in the resultant velocity can be seen when the Hartmann number M is magnified, as is to be expected. This is due to the conventional result, which states that the Lorentz energy is evidently due to the magnetic field's contribution, which rises to the opposing category of force just before the electrically conducting fluid. Following these qualities, in our study, the fluid stream motions in the thrust border stratum thicknesses eventually reached a point where they slowed down. The effects of the Grashof number Gr on the primary and secondary speed profiles are shown in Figure 3. Because misinterpreted Gr principles can cause buoyancy forces to increase and viscous forces to decrease, Gr is used to evaluate the relationship between a fluid's thermal buoyancy and viscous force. The fluid's internal resistance will also reduce when the viscosity lowers, which will increase the fluid velocity. The results of the adjusted Grashof number Gm on both velocity distributions can be seen in Figure 4. The solutal Grashof number Gm calculates the ratio of buoyancy to viscous force acting on a fluid; raising Gm causes the buoyancy to rise and the viscous forces to decrease. The internal fluid resistance decreases, resulting in an increase in the fluid's speed.

In fact, it is obvious, observing Figure 5, that a rise in the permeability parameter k causes the secondary velocity to compress, leading to an increase in the principal velocity constituent u. The primary velocity component u increases significantly due to the consequences of the Hall current over the whole liquid region. It would appear that the higher

the quantity of k is, the higher the resultant speed is and, consequently, the greater the thickness of the momentum boundary layer is. The lower the penetrability is, the more likely it is that a smaller fluid velocity will be observed in the fluid's flow constituency. Figure 6 shows the secondary and main velocity curves of various rotation effects. These curves provide accessible information. It is clear from Figure 6 that as the value of R increases, the primary velocity (u) profile and the secondary velocity (v) profile both begin to decrease. The primary fluid velocity, in most cases, decreases as a result of rotation throughout the entire boundary layer region. However, v increases due to expanding R in the area surrounding the plate, while it decreases in the vicinity away from the shield. This is because the Coriolis force is particularly strong in the region that is located near the axis of the rotary motion.

Figure 7 shows how the velocity profiles behave when the Hall parameter is used. By raising the Hall constraint m across the fluid media, the principal velocity and secondary velocity are both improved. It was found that the motivation Frontier stratum thicknesses across all liquids section rose together with the resultant speed, which served as reinforcement in the Hall factor. The intensity of the renitent magnetic field is decreased by the integration of the Hall parameter since it reduces effective conduction. For example, the proper operation and generation of a Hall current depend on the ions' to electrons' relative mobility in MHD Hall generators. For ionised helium gas, this is the situation. I feel that the electron Hall parameter should be arbitrarily increased in value. boost a hall generator's efficiency, to the best of my understanding and intuition. the pertinent engineering and industrial applications of the Hall result include present changes, proximity sensing, speed detection, keyboard switches, computers, and Galaxy S4 accessories, tachometers, antilock brakes, magnetometers, DC motors, disc drives, and other existing sensor devices. Other uses include those for current sensing, speed detection, and proximity sensing. Figures 8 and 10 depict, respectively, how thermal radiation R affects the primary and secondary fluid velocities and the fluid temperature. Figures 8 and 10 make it abundantly evident that the thermal radiation lowers the system's temperature and velocity. According to physical principles, thermal radiation causes the fluid medium's temperature to drop, which in turn causes the liquid particles' kinetic energy to drop. The velocities of the fluids are thereby slowed down.

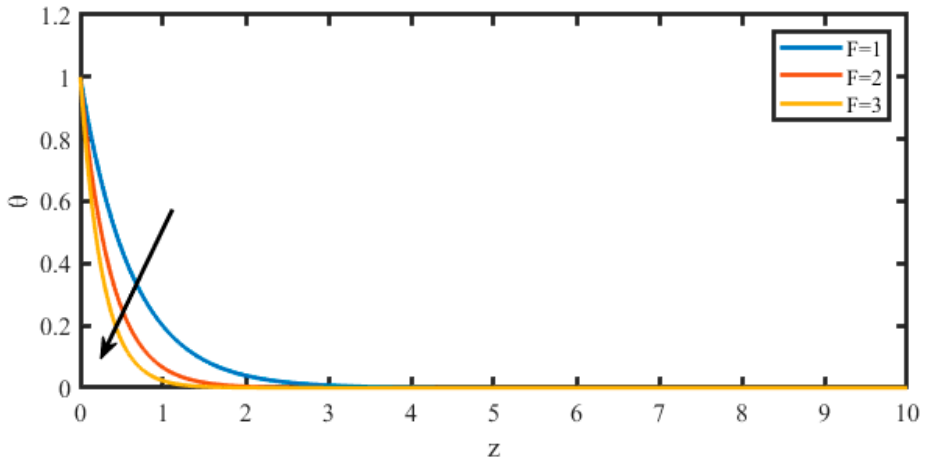

Figure 10. The influence of the radiation parameter F on the temperature profiles.

Soret number's impact on secondary fluid velocities are primary fluid velocities seen in Figure 9. Figure 9 clearly shows that when the Soret number, So, increases, so do u and v. This suggests that throughout the region of the boundary layer, the Soret number accelerates secondary and primary fluid velocities. A decrease in the mixture's viscosity is indicated by an increase in the number of Sorets. As a result, the effects of inertia and viscosity are enhanced. As a result, the velocity components grow. The impact of Prandtl number Pr on temperature profiles is shown in Figure 11. The ratio of thermal diffusiveness to kinematic

viscosity is known as the Prandtl number. A similar tendency is detected with an increase in H in Figure 12. According to what was predicted, increasing the value of H made the temperature differences less noticeable—Because temperature source parameters indicate Transfer of warm energy and temperature absorption. Because of this, the thicknesses of the layers that make up the heat frontier are decreased. Figure 13 Analyzes a chemical reaction's impact on concentration profiles. A destructive chemical process is examined in this study ($Kc > 0$). As chemical reactions increase, the distributions of concentration shrink. The chemistry is physically accompanied by characterized by many disturbances for a destructive purpose. Therefore, fluid flow concentration distributions are reduced as a result of high molecular motion, which increases transport phenomena.

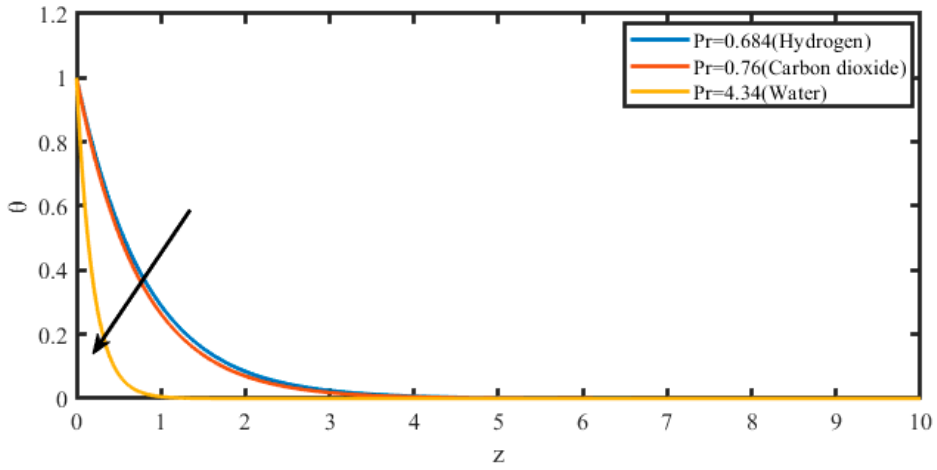

Figure 11. The influence of the Prandtl number parameter Pr on the temperature profiles.

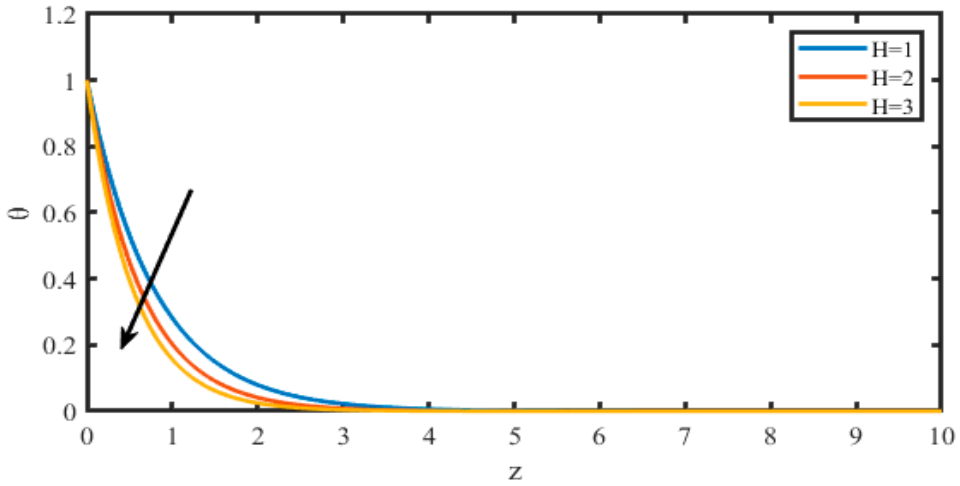

Figure 12. The influence of the Heat source parameter H on the temperature profiles.

Figure 14 demonstrates how the species concentration ϕ rises along with the number of Sorets. A rise in the Soret effect, by definition, indicates an increase in molar mass diffusivity. An increase in the increase in concentration is due to molecule mass diffusivity. This shows that the species concentration in the fluid tends to rise as the Soret number rises. Figure 15 illustrates the behavior of the Schmidt number (Sc) on the concentration curves. The momentum to mass diffusivity ratio is represented by the Schmidt number Sc. It determines the relative effectiveness of momentum and mass transmission by employing diffusion in the hydrodynamic (velocity & concentration) boundary layer. As well as the Schmidt number decreases, the fluid's mass diffusivity.

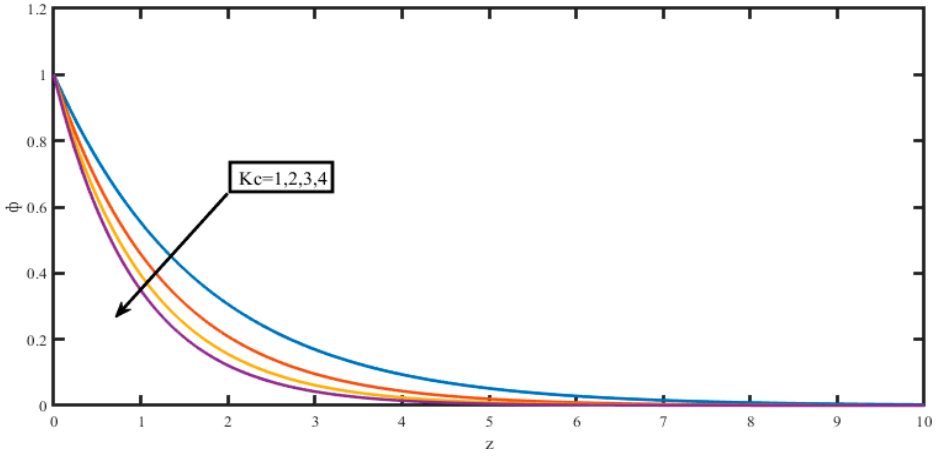

Figure 13. The influence of the Chemical reaction parameter *Kc* on the Concentration profiles.

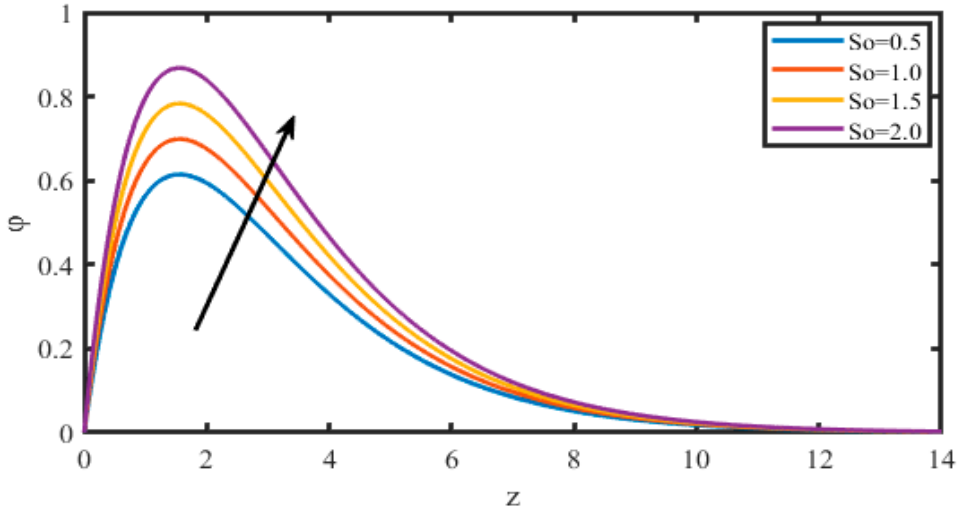

Figure 14. The influence of the Soret parameter *So* on the Concentration profiles.

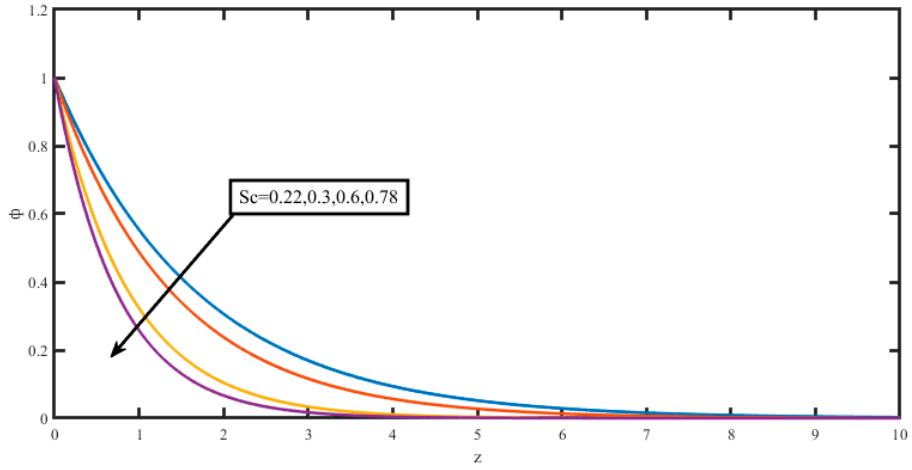

Figure 15. The influence of the Schmidt number *Sc* on the Concentration profiles.

The importance of skin friction is delineated in Table 1. An accumulation in the Hartmann portion will diminish the quantity of variance encountered by the skin fiction because of Lorentz's power decreases the friction and drag that it causes on gelatinous liquid. Examining the Prandtl number, the temperature source parameter, and an increase in the rotational parameter caused by the Coriolis force will reveal any similarities. By

increasing the penetrability parameter because of the drag force on the surface's border, the surface is also able to withstand greater skin friction.

Table 1. The shear stress.

M	*k*	*R*	**Pr**	*Gr*	*Gm*	*Sc*	*Kc*	*H*	*So*	*m*	*τ*
2.0	0.50	1.0	0.710	3.0	5.0	0.22	1.0	1.0	1.0	0.20	0.6248
3.0											0.7245
4.0											0.7645
	1.5										1.9475
	2.0										2.0657
		2.0									1.6578
		3.0									1.7458
			3.0								0.8542
			7.0								0.8154
				6							1.9875
				9							2.2547
					10						1.8752
					15						2.0124
						0.4					2.5479
						0.6					2.9875
							2.0				1.9875
							3.0				2.0214
								2.0			1.9647
								3.0			2.6578
									2.0		19875
									3.0		2.2448
										0.40	2.1254
										0.60	2.1004

An t = 5, = 0.5, = 0.5, = 0.01, = 0.5.

Table 2 lists the numerical various of the Nusselt number *Nu* that were calculated using the analytical expression for different values of Pr, *H*, *F*, *Kc*. Table 2 shows that the Nusselt number *Nu* grows as Pr, *H*, and *Kc* increase while decreasing as time *F* increases. This suggests that thermal radiation and diffusion both contribute to speed up the plate's heat exchange. Heat transfer speed to the plate decreases over time.

Table 3 lists the numerical the Sherwood number's values *Sh* that were calculated using the analytical equations for a mixture of values of *Sc*, *Kc*, *So* and t. Tab:3 shows that while the rate of mass transfer drops as *So* increases, it increases when *Sc*, *Kr* and *t* increase. This suggests that the rate of mass transfer at the plate is generally increased by mass diffusion, chemical response restriction, and time. The opposite is true for thermal radiation, thermal diffusion, and Soret number. The main speed results and the secondary rapidity outcome of Deepthi et al. [10] was in perfect agreement (Table 4).

Table 2. The Nusselt number (*Nu*).

Kc	*H*	*F*	Pr	*Nu*
1.0	1.0	1.0	0.710	0.445215
2.5				0.645214
3.5				0.712032
	2.5			1.578521
	3.5			1.945214
		2.5		0.978521
		3.5		0.978521
			3.5	3.478542
			7.5	7.578512

$A = 5.0$, $\epsilon = 0.010$, $Sc = 0.220$.

Table 3. The Sherwood number.

Kc	*Sc*	*So*	*T*	*F*	*Sh*
1.0	0.220	0.50	0.50	1.0	0.578521
2.5					0.645876
3.5					0.778521
	0.35				0.712014
	0.45				0.978520
		2.5			2.801234
		3.5			1.312478
			1.5		0.498741
			2.5		0.445214
				2.5	1.278521
				3.5	1.045210

$A = 5.0$, $\epsilon = 0.010$.

Table 4. The findings for the primary velocity compared and contrasted.

M	*K*	*Gr*	*Gm*	Previous Results Deepthi et al. [10]	Present Values
2.0	0.50	5.0	3.0	0.70785200	0.7458752
3.0				0.44587710	0.4785214
4.0				0.33254700	0.3785214
	1.00			0.75266440	0.7785214
	1.50			0.85657100	0.8021448
		10.0		0.97521200	0.9321477
		15.0		1.00214700	1.0785214
			6.0	0.76578280	0.7785214
			9.0	0.81032570	0.8654785

$A = 5.0$, $n = 0.50$, $t = 0.50$, $\epsilon = 0.010$, $U_0 = 0.50$, $m = 1.0$, $Sc = 0.220$, $Kc = H = 1.0$, and $So = 0$.

5. Conclusions

An examination of Hall's impact currents, turns, plus Soret numbers on top of an incompressible, viscous, electrically conductive second-order liquid that undergoes heat and mass relocates as it passes through a never-ending vertical plate set into a porous

media is presented. Correct results of the main equations were generated utilizing the regular perturbation method. Fluid velocity, heat, and species concentration are shown in fine-grained graphs, and their interactions with other physical variables are discussed.

Thermal removal energy tends to slow down the secondary liquid speed along the border line line coating area. The primary liquid speed tends to rise close to the plate due to the thermal buoyancy effect. Thus, the primary liquid speed changes direction in the area furthest from the shield. absorption buoyancy accelerates secondary and primary fluid velocities through the area of a boundary layer. Additionally, mass extinction has the opposite result across the entire border line sheet region. In the boundary layer region, the Hall current has the opposite effect on the primary fluid speed; there the secondary fluid tends to accelerate its velocity. Rotation increases the secondary liquid speed through the border line sheet section, although this often has the opposite effect. Due to the permeability of the porous material, the secondary fluid velocity often increases in the border line line plate section. However, the primary liquid speed is adversely affected in the boundary layer section. The Soret step finally increases both the boundary line layer region's primary and secondary liquid velocities. An expansion in the boundary layer's Soret number and time leads to an increase in species concentration. The effects of mass diffusion and heat energy slow down species concentrations. Skin friction is decreased by the Prandtl number, a hall current, and a concentration buoyancy force. The inverse is true for thermal buoyancy force, permeability, rotation, Soret number, chemical reaction, and mass diffusion. The heat relocates rate rises by means of the Prandtl number, heat source, and chemical reaction. Mass transfer rates are increased by chemical reaction, Schmidt number, and time, whereas they are decreased by heat radiation and Soret number.

Author Contributions: Conceptualization, O.T.B. and F.A.; methodology, K.R.; software, K.R.; validation, M.K., M.I.K. and K.G.; formal analysis, N.B.K.; investigation, E.S.M.T.-E.; resources, M.O.; data curation, F.A.; writing—original draft preparation, K.R. and F.A.; writing—review and editing, M.I.K.; visualization, M.O.; supervision, K.R. and M.I.K.; project administration, N.B.K.; funding acquisition, E.S.M.T.-E. All authors have read and agreed to the published version of the manuscript.

Funding: This research received no external funding.

Data Availability Statement: Not applicable.

Acknowledgments: The authors would like to thank the Deanship of Scientific Research at Umm Al-Qura University for supporting this work by Grant Code: 22UQU4340474DSR12.

Conflicts of Interest: The authors declare that they have no known competing financial interest or personal relationships that could have appeared to influence the work reported in this paper.

Abbreviations

Nomenclature

A	real positive constant
B_0	applied magnetic field (A/m)
x, y	dimensional co-ordinates (m)
u, v	velocity components in x and y directions (m/s)
C	non-dimensional fluid concentration (kg/m^3)
D_1	coefficient of thermal diffusivity (m^2 s^{-1})
g	acceleration due to gravity (m s^{-2})
Gr	thermal Grashof number
Gm	mass Grashof number
C_w	the uniform concentration of the fluid at the plate (kg m^{-3})
Kc	chemical reaction parameter (w/mk)
m	Hall parameter
C_∞	the concentration of the fluid far away from the plate (kg m^{-3})

Nomenclature

B	magnetic field vector (A/m)
q_w	local surface heat flux (W m^{-2})
Nu	local Nusselt number
E	electric field vector (c)
V	velocity vector (m/s)
k_1	thermal conductivity (W/m K)
K	permeability parameter
q_m	local surface mass flux (kg s^{-1} m^{-2})
P_e	electron pressure (Pascal)
Pr	Prandtl number
Sc	Schmidt number
J_x, J_y	current densities in x and y directions
k	permeability of porous medium (m^2)
H	heat source parameter
J	current density vector (A/m^2)
C_p	specific heat at a constant pressure (J/kg·K)
D	coefficient of mass diffusivity (m^2/s)
Sh	local Sherwood number
w	slip velocity (m s^{-1})
w_0	scale of suction velocity
So	Soret number
t	time (s)
u_0	plate velocity (m s^{-1})
q_r	radiative heat flux
F	radiation parameter (cm^{-2})
T_w	the uniform temperature of the fluid on the plate (K)
T_∞	the temperature of the fluid far away from the plate (K)
R	rotation parameter
S	second grade fluid
M	Hartmann number
N	constant

Greek symbols

β	coefficient of thermal expansion of the fluid
Ω	angular velocity (s^{-1})
τ_w	local wall shear stress (pascal)
τ_e	electron collision time (s)
ω_e	cyclotron frequency (e/mB)
ϕ	non-dimensional concentration (mol/m^3)
v	kinematic viscosity (m^2/s)
τ	local skin friction coefficient
β *	coefficient of mass expansion of the solid
Θ	non-dimensional temperature (K)
ρ	fluid density (Kg/m^3)
σ	electrical conductivity (S/m)

Subscripts and Superscripts

∞	free stream conditions
i	ions
w	conditions on the wall
e	electrons

References

1. Bestman, A.R.; Adjepong, S.K. Unsteady hydromagnetic free-convection flow with radiative heat transfer in a rotating fluid. *Astrophys. Space Sci.* **1998**, *143*, 73. [CrossRef]
2. Mbeledogu, I.U.; Ogulu, A. Heat and Mass Transfer of an Unsteady MHD Natural Convection Flow of a Rotating Fluid Past a Vertical Porous Flat Plate in the Presence of Radiative Heat Transfer. *Int. J. Heat Mass Transf.* **2007**, *50*, 1902–1908. [CrossRef]
3. Seth, G.S.; Nandkeolyar, R.; Ansari, M.S. Effects of Thermal Radiation and Rotation on Unsteady Hydromagnetic Free Convection Flow past an Impulsively Moving Vertical Plate with Ramped Temperature in a Porous Medium. *J. Appl. Fluid Mech.* **2013**, *6*, 27.
4. Sutton, G.W.; Sherman, A. *Engineering Magnetohydrodynamics*; McGraw-Hill: New York, NY, USA, 1965.
5. Sarkar, B.C.; Das, S.; Jana, R.N. Hall Effects on Unsteady MHD Free Convective Flow Past an Accelerated Moving Vertical Plate with Viscous and Joule Dissipations. *Int. J. Comput. Appl.* **2013**, *70*, 19–28.
6. Seth, G.S.; Hussain, S.M.; Sarkar, S. Effects of Hall current and rotation on unsteady MHD natural convection flow with heat and mass transfer past an impulsively moving vertical plate in the presence of radiation and chemical reaction. *Bulg. Chem. Commun.* **2014**, *46*, 704–718.
7. Farhad, A.; Norzieha, M.; Sharidan, S.; Khan, I.; Sami, U.H. Hydromagnetic rotating flow in a porous medium with slip condition and Hall current. *Int. J. Phys. Sci.* **2012**, *7*, 1540–1548. [CrossRef]
8. Raghunath, K.; Mohanaramana, R. Hall, Soret, and rotational effects on unsteady MHD rotating flow of a second-grade fluid through a porous medium in the presence of chemical reaction and aligned magnetic field. *Int. Commun. Heat Mass Transf.* **2022**, *137*, 106287. [CrossRef]
9. Raghunath, K.; Mohanaramana, R.; Nagesh, G.; Charankumar, G.; Khan, S.U.; Khan, M.I. Hall and ion slip radiative flow of chemically reactive second grade through porous saturated space via perturbation approach. *Waves Random Complex Media* **2022**. [CrossRef]
10. Deepthi, V.V.L.; Lashin, M.M.A.; Kumar, N.R.; Raghunath, K.; Ali, F.; Oreijah, M.; Guedri, K.; Tag-ElDin, E.S.M.; Khan, M.I.; Galal, A.M. Recent Development of Heat and Mass Transport in the Presence of Hall, Ion Slip and Thermo Diffusion in Radiative Second Grade Material: Application of Micromachines. *Micromachines* **2022**, *13*, 1566. [CrossRef]
11. Bhattacharyya, K.; Mukhopadhyay, S.; Layek, G.C.; Pop, I. Effects of thermal radiation on micropolar fluid flow and heat transfer over a porous shrinking sheet. *Int. J. Heat Mass Transf.* **2012**, *55*, 2945–2952. [CrossRef]
12. Hussain, M.; Ashraf, M.; Nadeem, S.; Khan, M. Radiation effects on the thermal boundary layer flow of a micropolar fluid towards a permeable stretching sheet. *J. Frankl. Inst.* **2013**, *350*, 194–210. [CrossRef]
13. Oahimire, J.I.; Olajuwon, B.I. Effect of Hall current and thermal radiation on heat and mass transfer of a chemically reacting MHD flow of a micropolar fluid through a porous medium. *J. King Saud Univ. Eng. Sci.* **2014**, *26*, 112–121. [CrossRef]
14. Mabood, F.; Ibrahim, S.M.; Rashidi, M.M.; Shadloo, M.S.; Lorenzini, G. Non-uniform heat source/sink and Soret effects on MHD non-Darcian convective flow past a stretching sheet in a micropolar fluid with radiation. *Int. J. Heat Mass Transf.* **2016**, *93*, 674–682. [CrossRef]
15. Raghunath, K.; Charankumar, G.; Giulio, L. Effects of Soret, Rotation, Hall, and Ion Slip on Unsteady MHD Flow of A Jeffrey Fluid Through A Porous Medium in The Presence of Heat Absorption and Chemical Reaction. *J. Mech. Eng. Res. Dev.* **2022**, *45*, 80–97.
16. Obulesu, M.; Raghunath, K.; Reddy, P.M.; Charankumar, G.; Giulio, L.; Sidik, N.A.C. Unsteady MHD on Convective Flow of a Newtonian Fluid Past an Inclined Plate in Presence of Chemical Reaction with Radiation Absorption and Dufour Effects. *CFD Lett.* **2022**, *14*, 62–76. [CrossRef]
17. Nagesh, G.; Raghunath, K. Soret Radiation and Chemical Reaction effect on MHD Jeffrey fluid flow past an inclined vertical plate Embedded in porous medium. *MATERIALS Today Proc.* **2022**, *50 Pt 5*, 2218–2226. [CrossRef]
18. Muthucumaraswamy, R. Effects of a chemical reaction on a moving isothermal vertical surface with suction. *Acta Mech.* **2002**, *155*, 65–70. [CrossRef]
19. Ajibade, A.O.; Umar, A.M. Effect of chemical reaction and radiation absorption on the unsteady MHD free convection Couette flow in a vertical channel filled with porous materials. *Afr. Mat.* **2016**, *27*, 201–213. [CrossRef]
20. Raghunath, K.; Nagesh, G.; Reddy, V.R.C.; Obulesu, M. Unsteady MHD fluid flow past an inclined vertical porous plate in the presence of chemical reaction with aligned magnetic field, radiation, and Soret effects. *Heat Transf.* **2021**, *51*, 2742–2760. [CrossRef]
21. Raghunath, K.; Obulesu, M. Unsteady MHD oscillatory Casson fluid flow past an inclined vertical porous plate in the presence of chemical reaction with heat absorption and Soret effects. *Heat Transf.* **2022**, *51*, 733–752. [CrossRef]
22. Raghunath, K.; Obulesu, M.; Sujatha, S.; Venkateswaraju, K. Investigation of MHD Casson fluid flow past a vertical porous plate under the influence of thermal diffusion and chemical reaction. *Heat Transf.* **2022**, *51*, 377–394. [CrossRef]
23. Reddy, V.R.; Raghunath, K.; Obulesu, M. Characteristics of MHD Casson fluid past an inclined vertical porous plate. *Mater. Today Proc.* **2022**, *49*, 2136–2142. [CrossRef]
24. Ibrahim, F.; Elaiw, A.; Bakr, A. Effect of the chemical reaction and radiation absorption on the unsteady MHD free convection flow past a semi infinite vertical permeable moving plate with heat source and suction. *Commun. Nonlinear Sci. Numer. Simul.* **2008**, *13*, 1056–1066. [CrossRef]
25. Kesavaiah, D.C.; Satyanarayana, P.; Venkataramana, S. Effects of the chemical reaction and radiation absorption on an unsteady MHD convective heat and mass transfer flow past a semi-infinite vertical permeable moving plate embedded in a porous medium with heat source and suction. *Int. J. Appl. Math. Mech.* **2011**, *7*, 52–69.

26. Narayana, P.V.S.; Venkateswarlu, B.; Venkataramana, S. Effects of Hall current and radiation absorption on MHD micropolar fluid in a rotating system. *Ain Shams Eng. J.* **2013**, *4*, 843–854. [CrossRef]
27. Seth, G.S.; Mahato, G.K.; Sarkar, S. Effects of Hall current and rotation on MHD natural convection flow past an impulsively moving vertical plate with ramped temperature in the presence of thermal diffusion with heat absorption. *Int. J. Energy Tech.* **2013**, *5*, 1–12.
28. Seth, G.S.; Sarkar, S.; Hussain, S.M. Effects of Hall current, radiation and rotation on natural convection heat and mass transfer flow past a moving vertical plate. *Ain Shams Eng. J.* **2014**, *5*, 489–503. [CrossRef]
29. Takhar, H.S.; Chamkha, A.J.; Nath, G. MHD flow over a moving plate in a rotating fluid with magnetic field, Hall currentand free stream velocity. *Int. J. Eng. Sci.* **2002**, *40*, 1511–1527. [CrossRef]
30. Cramer, K.P.; Pai, S.I. *Magneto Fluid Dynamics for Engineers and Applied Physics*; McGraw-Hill Book Co: New York, NY, USA, 1973.
31. Grief, G.; Habib, I.S.; Lin, L.C. Laminar convection of a radiating gas in a vertical channel. *J. Fluid Mech.* **1971**, *45*, 513–520. [CrossRef]
32. Cowling, G.S. *Magneto Hydrodynamics*; Interscience Publishers: New York, NY, USA, 1957.
33. Abbasi, A.; Farooq, W.; Tag-ElDin, E.S.M.; Khan, S.U.; Khan, M.I.; Guedri, K.; Elattar, S.; Waqas, M.; Galal, A.M. Heat transport exploration for hybrid nanoparticle (Cu, Fe_3O_4)-based blood flow via tapered complex wavy curved channel with slip features. *Micromachines* **2022**, *13*, 1415. [CrossRef]
34. Waqas, H.; Oreijah, M.; Guedri, K.; Khan, S.U.; Yang, S.; Yasmin, S.; Khan, M.I.; Bafakeeh, O.T.; Tag-ElDin, E.S.M.; Galal, A.M. Gyrotactic motile microorganisms impact on pseudoplastic nanofluid flow over a moving Riga surface with exponential heat flux. *Crystals* **2022**, *12*, 1308. [CrossRef]
35. Shahid, M.; Javed, H.M.A.; Ahmad, M.I.; Qureshi, A.A.; Khan, M.I.; Alnuwaiser, M.A.; Ahmed, A.; Khan, M.A.; Tag-Eldin, E.; Shahid, A.; et al. A brief assessment on recent developments in efficient electrocatalytic Nitrogen reduction with 2D non-metallic nanomaterials. *Nanomaterials* **2022**, *12*, 3413. [CrossRef]
36. Manzoor, N.; Qasim, I.; Khan, M.I.; Ahmed, M.W.; Guedri, K.; Bafakeeh, O.T.; Tag-Eldin, E.S.M.; Galal, A.M. Antibacterial applications of low pressure plasma on degradation of multidrug resistant V. Cholera. *Appl. Sci.* **2022**, *12*, 9737. [CrossRef]
37. Mamatha, S.U.; Devi, R.L.V.R.; Ahammad, N.A.; Shah, N.A.; Rao, B.M.; Raju, C.S.K.; Khan, M.I.; Guedri, K. Multi-linear regression of triple diffusive convectively heated boundary layer flow with suction and injection: Lie group transformations. *Int. J. Mod. Phys. B*, 2022; *in press*. [CrossRef]
38. Kiranakumar, H.V.; Thejas, R.; Naveen, C.S.; Khan, M.I.; Prasanna, G.D.; Reddy, S.; Oreijah, M.; Guedri, K.; Bafakeeh, O.T.; Jameel, M. A review on electrical and gas-sensing properties of reduced graphene oxide-metal oxide nanocomposites. *Biomass Convers. Biorefinery*, 2022; *in press*. [CrossRef]